37. B. D. Tapley, S. Bettadpur, J. C. Ries, P. F. Thompson, M. M. Watkins, *Science* **305**, 503 (2004).
38. We thank W. Abdalati, B. Chao, J. Dickey, W. Munk, and J. Zwally for helpful information; D. Cain for technical assistance; and J. Kaye, D. Anderson, P. DeCola, T. Lee, and E. Lindstrom (NASA Earth Science Research Division managers) and H. Harvey (Hewlett Foundation) for research support. These data were collected and made freely available by the International Argo Project and the national programs that contribute to it (www.argo.ucsd.edu, http://argo.jcommops.org). Argo is a pilot program of the Global Ocean Observing System.

Supporting Online Material
www.sciencemag.org/cgi/content/full/1110252/DC1
SOM Text
Figs. S1 and S2
Table S1
References

26 January 2005; accepted 19 April 2005
Published online 28 April 2005;
10.1126/science.1110252
Include this information when citing this paper.

Anchorless Prion Protein Results in Infectious Amyloid Disease Without Clinical Scrapie

Bruce Chesebro,[1]* Matthew Trifilo,[2] Richard Race,[1] Kimberly Meade-White,[1] Chao Teng,[2] Rachel LaCasse,[1] Lynne Raymond,[1] Cynthia Favara,[1] Gerald Baron,[1] Suzette Priola,[1] Byron Caughey,[1] Eliezer Masliah,[3] Michael Oldstone[2]

In prion and Alzheimer's diseases, the roles played by amyloid versus nonamyloid deposits in brain damage remain unresolved. In scrapie-infected transgenic mice expressing prion protein (PrP) lacking the glycosylphosphatidylinositol (GPI) membrane anchor, abnormal protease-resistant PrPres was deposited as amyloid plaques, rather than the usual nonamyloid form of PrPres. Although PrPres amyloid plaques induced brain damage reminiscent of Alzheimer's disease, clinical manifestations were minimal. In contrast, combined expression of anchorless and wild-type PrP produced accelerated clinical scrapie. Thus, the PrP GPI anchor may play a role in the pathogenesis of prion diseases.

Transmissible spongiform encephalopathies (TSEs) or prion diseases (*1*) include Creutzfeldt-Jakob disease (CJD) in humans, bovine spongiform encephalopathy or "mad cow dissease" in cattle, scrapie in sheep, and chronic wasting disease in deer and elk of North America. These diseases are similar to nontransmissible protein deposition diseases, such as the systemic amyloidoses and Alzheimer's disease, where a host-derived protein is misfolded and persists in an aggregated form that may damage nearby cells. Amyloid may be present in all these diseases; however, there are important differences among these disease families. In systemic amyloidoses, amyloid deposits in organs appear to be directly pathogenic (*2*), whereas in Alzheimer's disease, pre-amyloid forms (rather than amyloid itself) may be the major neuropathogenic moiety (*3*, *4*). In prion diseases, amyloid formation is variable and may contribute to pathogenesis (*5*). The host protein involved in misfolding and amyloid formation is PrP (*6*, *7*), and PrP is required for susceptibility to disease as well as replication of infectivity (*8*). After infection, normal protease-sensitive PrP (PrPsen) is converted to an aggregated partially protease-resistant structure (PrPres or PrP^{Sc}) (*9*) associated with brain pathology. Three basic patterns of PrPres deposition are found in prion diseases: diffuse "synaptic" nonamyloid deposits, coarse perivacuolar deposits, and dense plaque-like amyloid deposits (*10*, *11*). However, the relative roles of these PrPres forms in brain tissue damage are unknown.

In most cell types, the majority of PrPsen is expressed as a GPI-linked cell surface glycoprotein (*12*), but the role of this GPI membrane anchor in TSE disease is unclear. In cell-free experiments, PrP lacking the GPI moiety ("anchorless PrP") can be converted to the PrPres form (*13*, *14*). However, in scrapie-infected cells, absence of the GPI moiety reduces conversion (*15*, *16*), which suggests that conversion involves membrane-bound GPI-linked PrP. However, redirecting PrP to clathrin-coated pits on the plasma membrane by fusing PrP to a transmembrane domain blocks conversion to PrPres (*17*). Thus, GPI-negative (GPI^-) PrP might facilitate or inhibit susceptibility to TSE infection in vivo. Here, we tested the role of the PrP GPI anchor in scrapie infection and disease in transgenic mice expressing only GPI^- PrP.

Generation of GPI-negative PrP transgenic mice. The transgene was constructed by modifying the ''half-genomic'' mouse PrP plasmid pHGPrP (fig. S1) (*18*). Two transgenic (Tg) lines expressing the highest amounts of PrP (Tg23 and Tg44) were selected for experiments. In brains of Tg23 and Tg44 lines heterozygous for the transgene, PrP mRNA expression was half that in C57BL/6 control mice. Organ extracts were also analyzed for PrPsen expression. In brain, PrPsen levels were about one-fourth that in controls, and PrP was also noted in several other tissues (Fig. 1A). The protein was mainly in the unglycosylated form. In neurons isolated from Tg44 mice, PrP was not located on the cell surface, as is the case with GPI-linked PrP (Fig. 1B). However, levels of intracellular PrP in these mice were similar to controls, indicating that PrP did not accumulate abnormally in these cells. In floatation gradients using brain tissue, GPI^- PrP did not float with raft fractions, in contrast to wild-type GPI-linked PrP (fig. S2). In cell lines, GPI^- PrP was not detectable on the plasma membrane (fig. S3) but appeared in the endoplasmic reticulum and Golgi complex, and was secreted into the medium (*19*). Thus, GPI^- PrP differed markedly from wild-type PrP in subcellular localization and processing.

Infection with three scrapie strains. To study the susceptibility of GPI^- PrP Tg mice to scrapie infection, we inoculated Tg mice and non-Tg controls intracerebrally at 6 weeks of age with scrapie brain homogenate containing 0.7×10^6 to 1.0×10^6 ID_{50} (where ID_{50} is the dose causing disease in 50% of animals). Three scrapie strains [RML (Chandler), ME7, and 22L] (*20*, *21*) were tested to assess strain-dependent differences. Mice were observed daily for typical clinical signs of scrapie, including altered gait, kyphosis, ataxia, disorientation, somnolence, and wasting (Table 1). Clinical disease occurred within 140 to 160 days in control mice homozygous for endogenous wild-type mouse PrP, and within 240 to 260 days in heterozygous control mice. In contrast, in Tg23 and Tg44 mice, no clinical signs were observed after 600 days with the RML strain or 400 days with the ME7 strain. Two 22L-infected mice from line 23 developed a wasting syndrome without neurological signs and died at 370 days. Two other mice in this group showed no symptoms of disease after more than 550 days (Table 1), whereas 22L-infected mice from line 44 showed no symptoms after more than 440 days. Thus, the wasting syndrome in line Tg23 was unlikely related to scrapie infection. In summary, scrapie infection failed to induce the usual clinical manifestations of prion disease in these Tg mice.

Replication of scrapie agent. The lack of clinical disease raised the issue of whether

[1]Laboratory of Persistent Viral Diseases, Rocky Mountain Laboratories, National Institute of Allergy and Infectious Diseases, Hamilton, MT 59840, USA. [2]Division of Virology, Department of Neuropharmacology, Scripps Research Institute, La Jolla, CA 92037, USA. [3]Departments of Neurosciences and Pathology, University of California, San Diego, La Jolla, CA 92093, USA.

*To whom correspondence should be addressed. E-mail: bchesebro@niaid.nih.gov

these Tg mice could replicate the scrapie agent. Therefore, scrapie-infected and mock-infected Tg mice were killed 20 to 291 days after inoculation, and brain samples were analyzed for infectivity. By titration in C57BL/6 mice, mock-infected Tg mice had no detectable infectivity. Infected Tg mice also had no detectable infectivity in brain (<500 ID_{50} per brain) at 20 to 30 days after infection. In contrast, at 120 to 291 days after infection, scrapie-infected Tg mice had titers ranging from 2×10^6 to 4.6×10^8 ID_{50} per brain (Table 2). This increase represented substantial scrapie replication relative to the amount inoculated (10^6 ID_{50}) and was more than five orders of magnitude higher than the level in brain at 20 to 30 days (Table 2). However, the highest titer seen was still about one-tenth the usual titer in non-Tg mice with clinical scrapie.

Because PrP sequence differences are known to influence relative susceptibility to scrapie infection, we also tested whether titration of infected Tg brain homogenates might be more sensitive if done in Tg mice. However, the Tg mice proved to be less sensitive than wild-type mice in these titrations, because none of the eight mice developed PrPres or became ill during 500 days of observation.

Detection of PrPres. To determine whether disease-associated PrPres was present, we examined brain homogenates of infected Tg mice by immunoblotting after treatment with proteinase K (PK). Mock-infected mice showed no development of PrPres up to 500 days. In contrast, mice infected with RML scrapie had detectable PrPres by immunoblot starting at day 213, and the signal continued to increase over the ensuing months (Fig. 1, C and D). Several Tg mice inoculated with RML scrapie had up to 40% more PrPres than usually found in the brains of clinically sick scrapie-infected non-Tg control mice (Fig. 1C). Thus, the lack of clinical signs of scrapie suggested that PrPres in these mice had a reduced level of toxicity.

Comparison of PrPres from Tg and non-Tg mice revealed similar resistance to PK digestion and a similar decrease in molecular mass of 6 to 7 kD after PK treatment, consistent with cleavage around residue 89 (Fig. 1E) (*7*, *22*, *23*). In some familial human prion diseases, PrP molecules present in PrPres are also truncated at the C terminus (*24*). However, analysis with antibodies directed to C-terminal PrP residues showed no evidence for truncation (Fig. 1F). After removal of carbohydrates with peptide:*N*-glycosidase F (PNGase F), the predominant PrP band seen was a fragment extending approximately between residues 89 and 231.

Detection of PrPres amyloid in brain tissue. In prion diseases, the deposition pattern and location of PrPres in brain are important aspects of the pathogenic process. To assess brain PrPres deposition, we examined scrapie-infected Tg mice histologically. Dense plaque-like PrPres deposits were detected in the corpus callosum as early as 70 days after infection with scrapie strain RML (Fig. 2A). From day 213 onward there was a progressively wider distribution of PrPres deposits extending to the cerebral cortex, hippocampus, fimbria, hypothalamus, and forebrain (Fig. 2, B to D). PrPres was often near blood vessels (Fig. 2B, inset) and accumulated in dense deposits (Fig. 2E, right), unlike the diffuse PrPres seen in scrapie-infected non-Tg mice (Fig. 2E, left). By 419 days after inoculation, vacuolation typical of prion disease was seen in white matter areas (Fig. 2F). After 22L infection, dense PrPres plaques were found not only in the corpus callosum (Fig. 2G) but also in the cerebellum and brainstem (Fig. 2H) (fig. S3). The ability of strain 22L to infect the cerebellum was also noted in non-Tg mice; this appeared to be a strain-specific property (*25*) not altered by the presence or absence of PrP an-

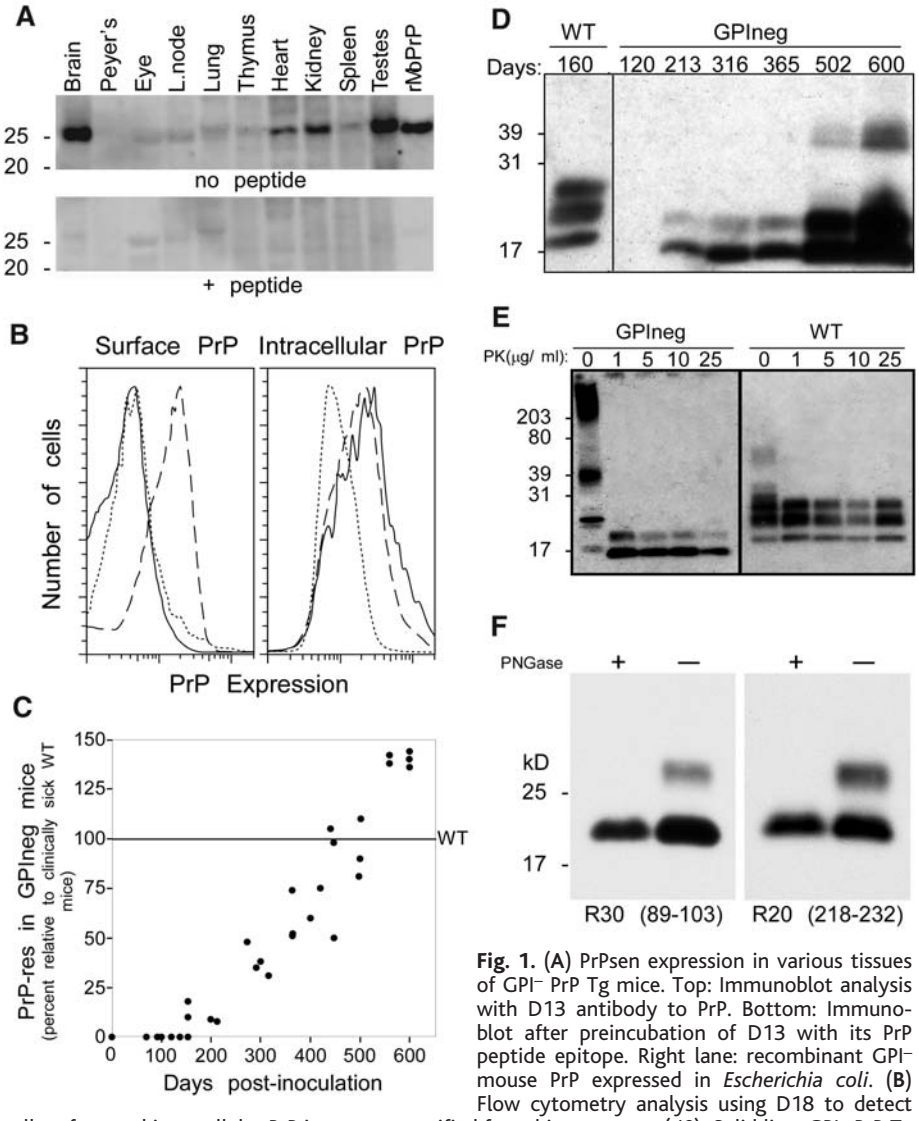

Fig. 1. (**A**) PrPsen expression in various tissues of GPI⁻ PrP Tg mice. Top: Immunoblot analysis with D13 antibody to PrP. Bottom: Immunoblot after preincubation of D13 with its PrP peptide epitope. Right lane: recombinant GPI⁻ mouse PrP expressed in *Escherichia coli*. (**B**) Flow cytometry analysis using D18 to detect cell surface and intracellular PrP in neurons purified from hippocampus (*40*). Solid line, GPI⁻ PrP Tg mouse (Tg44); dashed line, C57BL/6 control mouse; dotted line, PrP null (−/−) mouse. GPI⁻ PrP Tg mice have normal intracellular PrP expression but lack cell surface expression, in agreement with findings that GPI⁻ PrP is secreted from cells (*19*). (**C**) PrPres in brain of scrapie-infected GPI⁻ PrP Tg mice as a percentage of the amount in wild-type mice with clinical scrapie. After 500 days, PrPres in asymptomatic Tg mice exceeded the amount in diseased wild-type mice. (**D**) Immunoblot analysis of PrPres in brains of individual GPI⁻ PrP Tg mice at various days after scrapie inoculation. Brain homogenate from clinically ill wild-type mice is shown for comparison. (**E**) Proteinase K sensitivity of PrPres found in GPI⁻ PrP Tg mice. PrPres in Tg and non-Tg control mice have similar PK sensitivity. Species of higher molecular mass in lanes without PK in brain extracts from Tg mice indicate presence of PrP multimers, not prominent in infected non-Tg control mice. (**F**) Immunoblotting of PrPres from scrapie-infected GPI⁻ PrP Tg mouse before and after treatment with PNGase F to remove carbohydrates. Blotting with antibodies directed to PrP residues 89 to 103 (R30) or 218 to 232 (R20) gave identical patterns; this result indicates that the PrPres is not prematurely truncated at the C terminus, as is PrP amyloid in human familial prion disease.

choring. Strain ME7 was similar to 22L but did not induce PrPres in the cerebellum (table S1).

Because the dense deposits of PrPres appeared to be plaque-like in nature, brains of infected mice were stained with thioflavin S to test for amyloid plaque formation. Tg mice infected with RML, 22L, or ME7 scrapie strains showed very bright staining with thioflavin S in all areas positive for PrPres (Fig. 2, I and J), whereas PrPres in non-Tg mice infected with these same strains was negative. Thus, PrPres in Tg mice appeared predominantly in the form of amyloid plaques, in contrast to PrPres in non-Tg control mice where minimal amyloid was found.

Electron microscopic studies. To confirm that the thioflavin S staining seen by light microscopy was associated with fibrillary protein deposits typical of amyloid, we used electron microscopy to examine brains of scrapie-infected Tg mice. After infection of Tg mice, ultrastructural abnormalities were seen in both gray and white matter, whereas uninfected and mock-infected Tg mice were identical to control mice. Abundant deposition of amyloid fibrils was observed both in and around vascular endothelial cells and was associated with hypertrophic contorted basement membranes (Fig. 3, B and C). Furthermore, in the corpus callosum, swollen dystrophic nonmyelinated axons containing abnormal lysosomes and other electron-dense bodies were found in the plaque regions (Fig. 3E). At the ultrastructural level, these lesions in scrapie-infected Tg mice were similar to lesions found in β-amyloid (Aβ) plaques of human patients with Alzheimer's disease or mouse models of Alzheimer's (*26*, *27*).

Coexpression of wild-type PrP and GPI-negative PrP accelerates scrapie disease. Previously, coexpression of a secreted PrP fusion protein plus wild-type PrP delayed scrapie disease in mice (*28*). Because PrP expressed in GPI$^-$ PrP Tg mice is also secreted from cells and is converted in cell-free reactions (*13*), we tested whether inhibition of scrapie would occur in mice coexpressing wild-type and GPI$^-$ PrP. After infection with strain 22L, non-Tg mice expressing only a single copy of the wild-type PrP gene died within 241 to 257 days. However, mice heterozygous for expres-

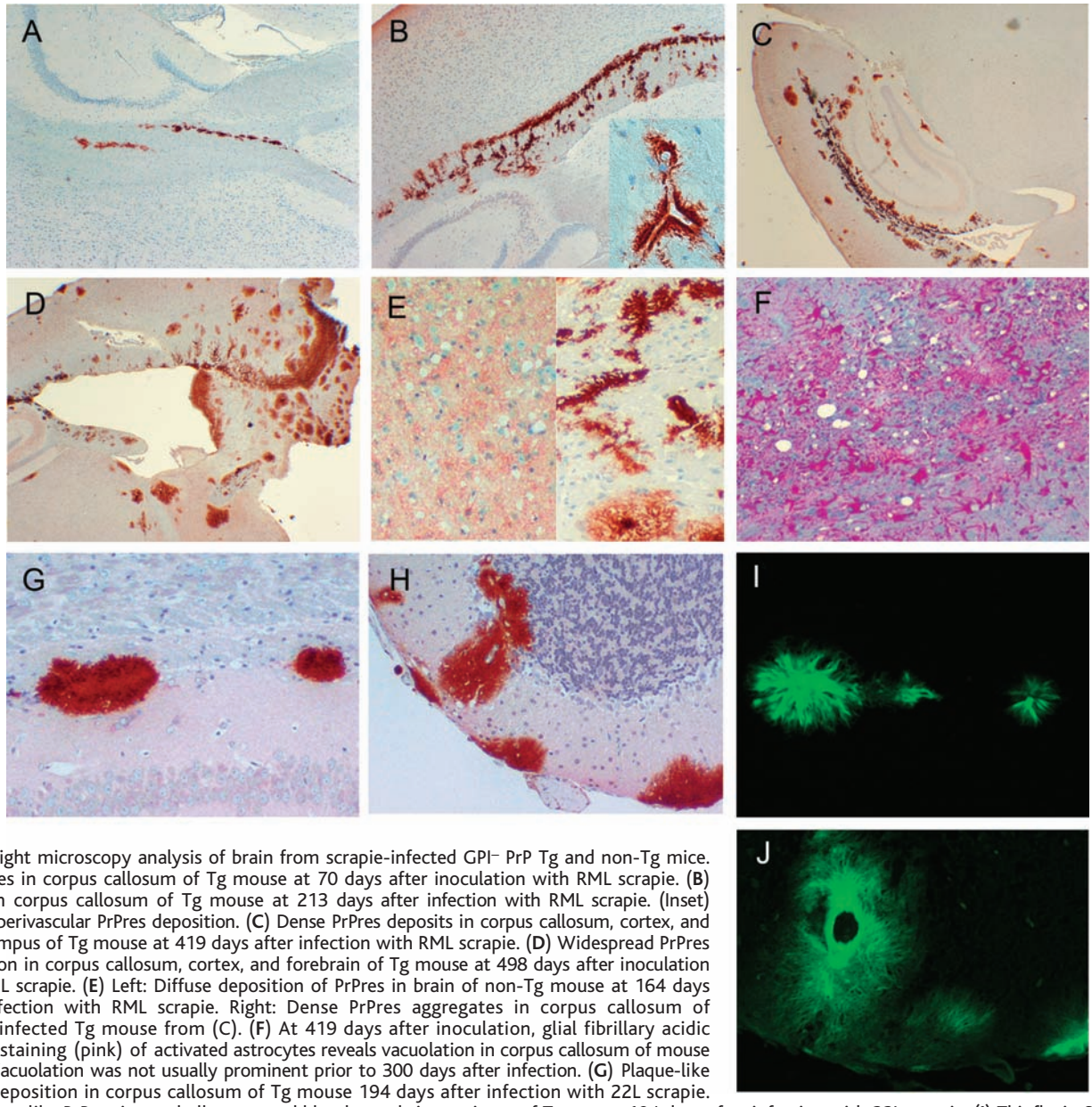

Fig. 2. Light microscopy analysis of brain from scrapie-infected GPI$^-$ PrP Tg and non-Tg mice. (**A**) PrPres in corpus callosum of Tg mouse at 70 days after inoculation with RML scrapie. (**B**) PrPres in corpus callosum of Tg mouse at 213 days after infection with RML scrapie. (Inset) Intense perivascular PrPres deposition. (**C**) Dense PrPres deposits in corpus callosum, cortex, and hippocampus of Tg mouse at 419 days after infection with RML scrapie. (**D**) Widespread PrPres deposition in corpus callosum, cortex, and forebrain of Tg mouse at 498 days after inoculation with RML scrapie. (**E**) Left: Diffuse deposition of PrPres in brain of non-Tg mouse at 164 days after infection with RML scrapie. Right: Dense PrPres aggregates in corpus callosum of scrapie-infected Tg mouse from (C). (**F**) At 419 days after inoculation, glial fibrillary acidic protein staining (pink) of activated astrocytes reveals vacuolation in corpus callosum of mouse in (C). Vacuolation was not usually prominent prior to 300 days after infection. (**G**) Plaque-like PrPres deposition in corpus callosum of Tg mouse 194 days after infection with 22L scrapie. (**H**) Plaque-like PrPres in cerebellum around blood vessels in meninges of Tg mouse 194 days after infection with 22L scrapie. (**I**) Thioflavin S staining of PrPres amyloid in corpus callosum of mouse in (G). (**J**) Thioflavin S staining of PrPres amyloid in cerebellum of mouse in (H). Magnifications: ×20 [(A) and (B)], ×10 [(C) and (D)], ×200 [(E) to (J)].

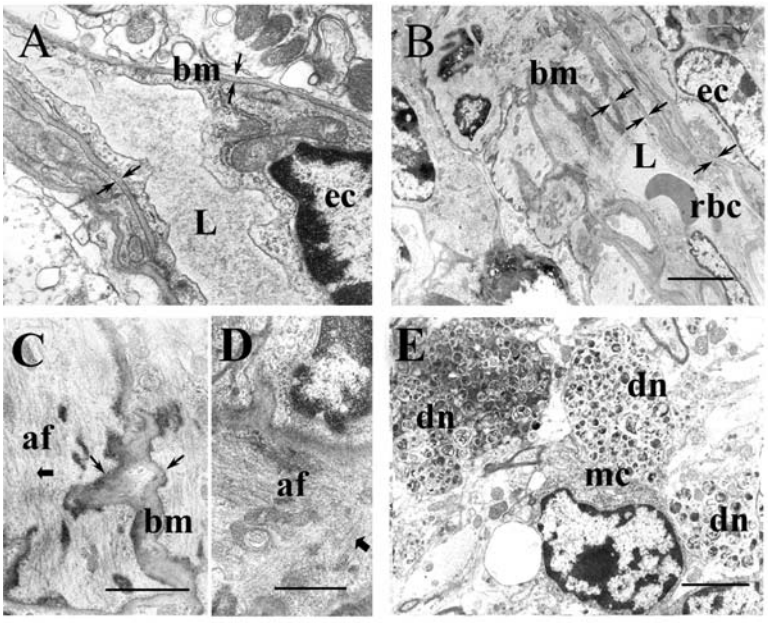

Fig. 3. Ultrastructural analysis of brains of scrapie-infected and uninfected GPI⁻ PrP Tg mice. Electron micrographs were obtained from the deep layers of the neocortex and corpus callosum. Infected mice were 400 days after infection with RML scrapie. (**A**) Low-power view of a normal brain blood vessel in uninfected mouse, showing the lumen (L) and adjacent endothelial cell [nucleus labeled (ec)]. Basement membrane (bm) is identified by arrows. (**B**) Low-power view of an intermediate-size brain blood vessel of scrapie-infected mouse displaying extensive disorganization of cytoarchitecture with distortion of the basement membranes (see arrows). Lumen of the vessel contains a red blood cell (rbc), and an adjacent endothelial cell nucleus is visible. Scale bar, 5 μm. (**C**) At higher magnification, entire perivascular space is packed with hair-like amyloid fibrils (af), and a single fibril is identified by a thick arrow. The basement membrane is irregular and thickened (thin arrows). Scale bar, 2 μm. (**D**) Extracellular amyloid fibrils (thick arrow) in perivascular region. Scale bar, 2 μm. (**E**) Neuritic plaque with microglial cell (mc) and three dystrophic nonmyelinated neurites (dn) containing abundant electron-dense and laminated bodies, similar to damage near Aβ amyloid plaques in human and mouse models of Alzheimer's disease. Scale bar, 4 μm.

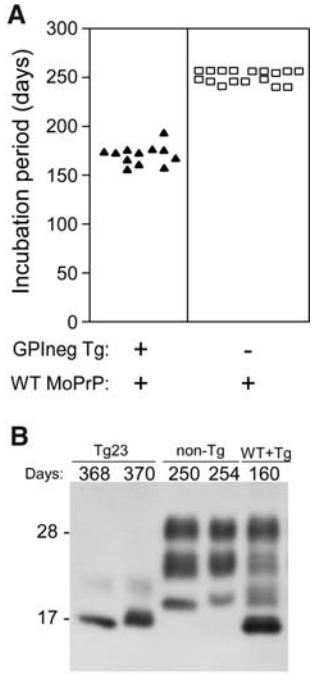

Fig. 4. (**A**) Acceleration of scrapie clinical disease in mice expressing both anchorless PrP and wild-type PrP. GPI⁻ PrP Tg (+/−) mice on the MoPrP (−/−) background were bred with non-Tg C57BL/10 mice previously selected to be heterozygous (+/−) for mouse PrP. Mice were infected with the 22L scrapie strain intracerebrally. All mice used were MoPrP heterozygous (+/−) and were separated into groups that were positive or negative for the GPI⁻ PrP transgene. Mice expressing both wild-type (WT) and GPI⁻ MoPrP developed clinical scrapie about 100 days earlier than mice expressing only WT MoPrP. (**B**) Immunoblot detection of PrPres in scrapie-infected Tg mice and control mice. Starting at left, lanes 1 and 2: Mice from Tg23 line inoculated with 22L scrapie died with wasting syndrome at 368 to 370 days. Lanes 3 and 4: Non-Tg littermate control mice heterozygous for mouse PrP (+/−) infected with 22L scrapie. Clinical disease with typical scrapie neurological signs was seen at 250 to 254 days after infection. Lane 5: Littermate control expressing both GPI⁻ PrP and WT PrP inoculated with 22L scrapie developed clinical disease at 160 days after inoculation. Each lane was loaded with 0.6 mg brain.

sion of both wild-type PrP and GPI⁻ PrP died within 156 to 192 days (Fig. 4A), and brains of these mice appeared to have PrPres generated from both PrP types (Fig. 4B). Thus, anchorless PrP accelerated rather than inhibited scrapie disease. The brains of these mice showed severe vacuolation plus a combination of diffuse PrPres and plaque-like PrPres, with a wider distribution of plaque-like PrPres than in mice expressing only anchorless PrP (fig. S3). The presence of both wild-type and anchorless PrP appeared to enhance the spread of both the amyloid and nonamyloid forms of PrPres.

Discussion. Deletion of the mouse PrP GPI anchor markedly changed the quality of PrPres found in brain, causing a shift from the usual diffuse or punctate nonamyloid pattern to a pattern with thioflavin S–positive PrPres amyloid. Thus, the GPI moiety might interfere with the ability of PrP to form amyloid fibrils. Possibly GPI-mediated PrP membrane attachment might account for this inhibition, or the GPI group might itself block the refolding necessary for amyloid formation. Alternatively, β-sheet structure and amyloid formation might be favored because GPI⁻ PrPsen mostly lacks carbohydrates. PrP amyloid found in humans with familial prion disease also lacks the GPI anchor and carbohydrates, but this amyloid PrP is truncated at both N and C termini, including removal of the entire second and third α helices (*24*, *29*). In contrast, the PrP amyloid found in Tg mice had no evidence for C-terminal truncation (Fig. 1F). Thus, the removal of the residues forming these helices was not as important as lack of the GPI group and the carbohydrates for PrP amyloid formation in vivo.

PrP is a required element for the replication of scrapie infectivity and development of disease (*8*). The present Tg mouse model has separated these aspects, as the GPI group of PrP strongly influenced the development of clinical disease with a lesser impact on agent replication. In GPI⁻ Tg mice, replication of infectivity occurred despite changes in the clinical disease and the type of PrPres deposits. However, relative to clinically ill wild-type mice, the amount of infectivity detected was reduced by nearly a factor of 10. These lower titers were not due to the presence of a new scrapie ''strain'' with a preference for mice expressing GPI⁻ PrP, because attempts to pass scrapie from Tg mice to recipient Tg mice were not successful. Thus, although the GPI anchor was not essential for replication of infectivity, the efficiency of replication in the context of anchorless PrP was reduced.

The lack of clinical disease induced by RML scrapie in the presence of PrPres amyloid and replication of scrapie infectivity is perhaps the most surprising aspect of the current Tg mouse model. PrP amyloid plaques did not cause a rapid fatal clinical disease similar to typical scrapie. Apparently, wild-type diffuse PrPres or its breakdown products are more toxic to brain function than is the amyloid PrPres seen in GPI⁻ PrP Tg mice. A similar hypothesis has been proposed for Alzheimer's disease where smaller Aβ protofibrils or peptides, rather than plaques, are thought by some to be the major pathogenic moieties (*3*, *4*). Alternative-

Table 1. Detection of clinical disease in scrapie-inoculated GPI$^-$ PrP Tg mice and non-Tg control (WT) mice. In proportions shown, the numerator is the number of mice developing clinical disease per total number of mice injected. The denominator represents the total number of mice under observation at the times indicated; this number was decreased at the times when mice were killed and was increased by inoculation of new mice in later experiments. WT non-Tg mice were either C57BL/6 or C57BL/10 mice.

Days	Proportion of positive mice									
	RML scrapie*				22L scrapie			ME7 scrapie		
	Tg23	Tg44	Tg50	WT	Tg23	Tg44	WT	Tg23	Tg44	WT
150	0/35	0/34	0/15	30/30	0/19	0/19	26/26	0/10	0/11	14/14
200	0/33	0/32	0/12		0/19	0/16		0/10	0/9	
250	0/30	0/28	0/10		0/19	0/16		0/10	0/9	
300	0/26	0/25	0/7		0/13	0/15		0/5	0/7	
400	0/13	0/20	0/3		2†/11	0/13		0/1	0/5	
500	0/5	0/2			2/4			0/1		
550	0/3	0/2			2/4			0/1		
600	0/2	0/1			2/4			0/1		

*Mock-infected Tg mice ($N = 8$) developed no clinical disease over a 500-day period. †These two mice developed a wasting syndrome without accompanying neurological signs, and they died at 370 days after inoculation.

Table 2. Titration of infectivity in brain tissue of scrapie-infected GPI$^-$ PrP Tg mice. Titer was calculated as ID_{50} per brain by dividing the 50% end-point dilution (determined by the Spearman-Karber method) by the volume inoculated (30 or 50 μl) and then multiplying by 400 mg, the average mouse brain weight.

Scrapie strain	Number of days after infection	Dilution of brain homogenate	Average incubation period (days)	Proportion of positive mice	Titer (ID_{50}/brain)
RML	20	5×10^1	>400	0/4	$<5.0 \times 10^2$
RML	30	5×10^1	>400	0/4	$<5.0 \times 10^2$
RML	120	5×10^2	180	6/6	
		5×10^4	200	3/3	
		5×10^5	230	3/3	4.6×10^8
		5×10^6	521	2/3	
		5×10^7	507	2/3	
		5×10^8	>550	0/3	
RML	291	5×10^2	160	7/7	
		5×10^3	180	3/3	2.0×10^6
		5×10^4	200	3/3	
		5×10^5	>400	0/3	
22L*	286	10^2	135	4/4†	
		10^3	158	4/4	
		10^4	173	4/4	$>2.4 \times 10^8$
		10^5	184	4/4	
		10^6	193	4/4	
		10^7	215	4/4	
Mock	120	5×10^1	>500	0/5‡	$<5.0 \times 10^2$

*This titration was initiated later and is still in progress. The titer given may be higher if more mice get sick at later times. †C57BL mice inoculated with brain homogenate from this 22L-infected GPI$^-$ PrP Tg mouse developed scrapie pathology and Western blot PrPres patterns similar to that induced by the original 22L scrapie preparation. ‡Single mice were killed at 330 and 500 days after infection and were negative by Western blot for PrPres. Three mice remained alive at 543 days with no signs of disease.

ly, the lack of normal membrane-anchored PrPsen in GPI$^-$ PrP Tg mice might reduce delivery of neurotoxic signals after PrPres formation (*30*, *31*). However, PrP-negative neurons can be damaged and killed indirectly by PrP-expressing astrocytes infected with scrapie strain 263K (*32*), although this process appears to be slower than when PrP-positive neurons are present (*33*).

The localization of the PrPres fibers and plaques around vascular endothelial cells in this model is similar to the PrP145 stop codon familial prion disease (*34*). We found amyloid fibrils both within endothelial cells and in adjacent extracellular locations, accompanied by basement membrane alterations (Fig. 3, B and C). Surprisingly, there was no evidence for increased expression of the transgene in brain endothelial cells (fig. S4). However, proteoglycans derived from endothelial cells might contribute to the observed perivascular deposition of PrPres, because sulfated proteoglycans similar to those present in basement membrane are known to bind PrPsen (*35*) and PrPres (*36*, *37*) and can even potentiate PrP conversion in vitro (*38*, *39*).

Despite the absence of obvious clinical disease, amyloid PrPres in brains of GPI$^-$ PrP Tg mice was associated with definite neuropathological lesions. By electron microscopy, dystrophic neurites were seen in association with amyloid fibrils and plaque-like lesions similar to Alzheimer's disease (*26*) (Fig. 3D). Because lesions were found primarily in the corpus callosum and only later in other areas, the lack of symptoms may be related to the locations of the lesions. Perhaps, beyond our current observation time of more than 600 days, extension of the 22L scrapie-induced lesions in the cerebellum or brainstem might produce more obvious symptomatology.

References and Notes

1. B. Chesebro, *Br. Med. Bull.* **66**, 1 (2003).
2. M. B. Pepys, *Philos. Trans. R. Soc. London Ser. B* **356**, 203 (2001).
3. B. Caughey, P. T. Lansbury, *Annu. Rev. Neurosci.* **26**, 267 (2003).
4. J. P. Cleary *et al.*, *Nat. Neurosci.* **8**, 79 (2005).
5. H. Fraser, M. Bruce, *Lancet* **i**, 617 (1973).
6. B. Chesebro *et al.*, *Nature* **315**, 331 (1985).
7. B. Oesch *et al.*, *Cell* **40**, 735 (1985).
8. H. Bueler *et al.*, *Cell* **73**, 1339 (1993).
9. K. Basler *et al.*, *Cell* **46**, 417 (1986).
10. H. Budka *et al.*, *Brain Pathol.* **5**, 459 (1995).
11. P. Parchi *et al.*, *Ann. Neurol.* **46**, 224 (1999).
12. N. Stahl, D. R. Borchelt, K. Hsiao, S. B. Prusiner, *Cell* **51**, 229 (1987).
13. D. A. Kocisko *et al.*, *Nature* **370**, 471 (1994).
14. V. A. Lawson, S. A. Priola, K. Wehrly, B. Chesebro, *J. Biol. Chem.* **276**, 35265 (2001).
15. B. Caughey, G. J. Raymond, *J. Biol. Chem.* **266**, 18217 (1991).
16. M. Rogers, F. Yehiely, M. Scott, S. B. Prusiner, *Proc. Natl. Acad. Sci. U.S.A.* **90**, 3182 (1993).
17. K. Kaneko *et al.*, *Proc. Natl. Acad. Sci. U.S.A.* **94**, 2333 (1997).
18. M. Fischer *et al.*, *EMBO J.* **15**, 1255 (1996).
19. M. Horiuchi, J. Chabry, B. Caughey, *EMBO J.* **18**, 3193 (1999).
20. R. L. Chandler, *Lancet* **1**, 1378 (1961).
21. M. E. Bruce, I. McConnell, H. Fraser, A. G. Dickinson, *J. Gen. Virol.* **72**, 595 (1991).
22. J. Hope *et al.*, *EMBO J.* **5**, 2591 (1986).
23. P. Parchi *et al.*, *Proc. Natl. Acad. Sci. U.S.A.* **97**, 10168 (2000).
24. F. Tagliavini *et al.*, *EMBO J.* **10**, 513 (1991).
25. M. E. Bruce, H. Fraser, *Curr. Top. Microbiol. Immunol.* **172**, 125 (1991).
26. E. Masliah *et al.*, *J. Neurosci.* **16**, 5795 (1996).
27. E. Masliah, A. Sisk, M. Mallory, D. Games, *J. Neuropathol. Exp. Neurol.* **60**, 357 (2001).
28. P. Meier *et al.*, *Cell* **113**, 49 (2003).
29. B. Ghetti *et al.*, *Brain Pathol.* **6**, 127 (1996).
30. S. Brandner *et al.*, *Nature* **379**, 339 (1996).
31. L. Solforosi *et al.*, *Science* **303**, 1514 (2004).
32. M. Jeffrey, C. M. Goodsir, R. E. Race, B. Chesebro, *Ann. Neurol.* **55**, 781 (2004).
33. G. Mallucci *et al.*, *Science* **302**, 871 (2003).
34. B. Ghetti *et al.*, *Proc. Natl. Acad. Sci. U.S.A.* **93**, 744 (1996).
35. B. Caughey, K. Brown, G. J. Raymond, G. E. Katzenstien, W. Thresher, *J. Virol.* **68**, 2135 (1994).
36. A. D. Snow, R. Kisilevsky, J. Willmer, S. B. Prusiner, S. J. DeArmond, *Acta Neuropathol. (Berlin)* **77**, 337 (1989).
37. P. A. McBride, M. I. Wilson, P. Eikelenboom, A. Tunstall, M. E. Bruce, *Exp. Neurol.* **149**, 447 (1998).
38. C. Wong *et al.*, *EMBO J.* **20**, 377 (2001).
39. O. Ben-Zaken *et al.*, *J. Biol. Chem.* **278**, 40041 (2003).
40. G. F. Rall *et al.*, *Proc. Natl. Acad. Sci. U.S.A.* **94**, 4659 (1997).

41. We thank S. Hughes, H. Lewicki, and K. Wehrly for laboratory technical assistance, and A. Mora and G. Hettrick for graphics assistance. Supported in part by NIH grant AG004342.

Supporting Online Material

www.sciencemag.org/cgi/content/full/308/5727/1435/DC1
Materials and Methods
Figs. S1 to S5

8 February 2005; accepted 4 April 2005
10.1126/science.1110837